Phasor Measurement Unit Incorporated Adaptive Out-of-step Protection of Synchronous Generator

Jigneshkumar P. Desai and Vijay H. Makwana

***Abstract*—The existing out-of-step (OOS) protection schemes have proven to be deficient in the prevention of significant outages. OOS protection schemes must not operate in stable power swing, and rapidly isolate an asynchronous generator or group of generators from the rest of the power system in case of unstable power swing. The paper proposes a novel phasor measurement unit (PMU) incorporating a polygon-shaped graphical algorithm for OOS protection of the synchronous generator. The unique PMU-based logic works further to classify the type of swing once the graphical scheme detects it, which can identify the complex power swing produced in the modern power system. The proposed algorithm can take the correct relaying decision in the event of power swing due to renewable energy integration, load encroachment, and transient faults. In this paper, the original and modified Kundur two-area system with a power system stabilizer (PSS) is used to test the proposed algorithm. In the end, it provides assessment results of the proposed relay on the Indian power system during the blackout in July 2012. The results demonstrate that the proposed algorithm is fast, accurate, and adaptive in the modern power system and shows better performance than the existing OOS protection schemes.**

***Index Terms*—Out-of-step protection, phasor measurement unit (PMU), power swing detection, renewable energy integration.**

I. Introduction

THE most common and inevitable disturbances of the power system are usually faults and sudden load changes. These disturbances lead to transient instability depending on their severity [1]. Power system stability plays a vital role in the reliable operation of the power system. The disturbances cause power oscillations, which are known as power swings [2]. Power swings can be synchronous (synchronous generators do not lose synchronism) or asynchronous (synchronous generators lose synchronism) depending on the severity of the disturbances [3]. At the generation side, when the generator or group of generators is exposed to the asynchronous power swing, instability may occur, and the generator experiences the pole slipping, which can cause stress on the system and pole (coil) [1]. Deep synchronous or asynchronous power swings are accompanied by massive changes in voltages and currents, which pose a serious threat to power system operation. An unstable power swing may cause mal-operation of some protection systems, especially distance protection and under-impedance protection, which, in turn, may lead to cascaded outages and blackouts [4]. For reliable operation, the out-of-step (OOS) protection scheme is provided, which has the following main elements [4]: ① special protection and supplementary control; ② power swing blocking (PSB) of distance protection; ③ pole slipping protection (PSP) of synchronous generators; ④ OOS tripping in transmission networks.

Nowadays, the power system integrated with photovoltaic (PV) generators leads to different transient events. The power swing characteristics of such a modern power system are complex compared with those of the power system in which only a synchronous generator is the primary source of power generation [1]. The penetration of PV and doubly-fed induction generator (DFIG) improves the damping of the system, but up to a certain level. If the penetration of solar PV is more than 50%, it creates a negative effect on the damping of the system [5]. The power system is generally protected against the power swing using the blinder-based OOS protection scheme. The method measures the change in impedance ΔZ to detect the OOS impedance trajectories [6]. The blinder-based relay may mal-operate for stable swing unless the user performs exact threshold estimation [7]. Furthermore, the blinder-based OOS relays require to improve with different renewable penetration levels. The increment of renewable power penetration into the existing power system can alter the coherent group of generators, swing frequency, and impedance trajectory. Furthermore, the increased penetration leads to timely changes in the OOS protection scheme [8]. The large-scale integration of wind generation changes the characteristics of power swing [9]. The PSB time delay requires frequent revision with increased penetration of wind power in the system. Reference [9] addresses the concern of protection improvements due to the negative impact of wind power generation, but does not reveal any proposed solution to the problem.

Reference [10] explains phasor measurement unit (PMU) application in the OOS protection. It uses direct phase angle comparison between different locations to identify the OOS

Manuscript received: April 30, 2020; accepted: September 14, 2020. Date of CrossCheck: September 14, 2020. Date of online publication: December 4, 2020.

J. P. Desai is with the Department of Electrical Engineering, Sarvajanik College of Engineering and Technology, Surat-395001, India, and he is also with Gujarat Technological University, Ahmedabad-382424, India (e-mail: jpd.fetr@gmail.com; 169999914003@gtu.edu.in).

V. H. Makwana is with the Department of Electrical Engineering, G. H. Patel College of Engineering and Technology, Anand-388120, India (e-mail: vijay911979@gmail.com).

DOI: 10.35833/MPCE.2020.000277

condition of the generator. However, it does not compare the proposed method with conventional OOS protection schemes such as double-blinder (DB) scheme.

Distance relays are most likely to be a pickup under the condition where the power swing arises on the transmission line [11]. The PMU signals, along with line inputs, are used to produce PSB signals under such conditions. The approach uses normalized minimum positive sequence voltage online as *y*-coordinate and positive sequence voltage angle as *x*-coordinate [11]. It presents a method for the OOS protection of line instead of the generator. The OOS protection of the generator is the most important during power swing, because recent advancement in power system moves the swing position away from the transmission line towards the generator and generator transformer [12]. Reference [13] presents an adaptive OOS relay logic. The angular separation is calculated and compared with the minimum and maximum angles. It checks the energy of the rotor simultaneously. Using all the information, it finds a stable or unstable power swing. Wide-area monitoring system (WAMS) in the network allows the real-time angular measurement to determine whether the system is going to collapse or remains stable [14]. However, the method in [14] uses the delays in the tripping of large generators, which may lead to damage in case of mal-operation of the scheme. The WAMS in [15] introduces the OOS splitting protection based on the information of voltage phase angle at each bus. The paper presents the technique that is not mathematically complex but relatively simple, which encourages the use of PMU for the OOS protection. In addition, the wide-area protection scheme for the prevention of widespread blackout is described in [16], which uses local signals available for distance relay and global signals from synchrophasor measurements. It is usually used for controlled islanding. The local and global signals can also be used to make the correct decision from OOS relays after sudden disturbance. Reference [17] proposes wide-area OOS prediction using an adaptively controlled islanding concept. A new adaptive OOS protection method is proposed in [17] and [18]. However, the method used for OOS protection in [17] and [18] is complex and must be verified with different levels of renewable penetration.

In this paper, we propose a novel solution, which overcomes the issues of OOS relay due to the impact of renewable integration, the usage of power sysytem stabilizer (PSS), the fault during power swing, the load encroachments, and the symmetrical faults. The proposed algorithm identifies the OOS generator or group of generators during asynchronous power swing events. In this paper, some underlying facts are observed during power swing using PMU measurements, which can detect unstable swing early regardless of system changes and configuration. The settings and threshold of the proposed algorithm do not require frequent revisions such as blinder-based relay. Thus, the proposed work significantly improves the OOS relay by providing pole slipping protection to a generator in the present power system. Section II explains the underlying facts during power swing using the mathematical analysis of PMU incorporated in a graphical OOS protection scheme. Section III explains the new algorithm steps and test system. Section IV shows the test cases for different stable and unstable power swings due to the symmetrical faults with PSS. In Section V, the performance of the proposed PMU-based polygon-shaped OOS protection scheme is described for the line-to-line (LL), line-to-ground (LG), and significant generator faults with the stable and unstable swings. A modified Kundur two-area system is used in Section VI to test the performance of the proposed OOS relay with the impact of renewable energy integration. Section VI also provides assessment results of the proposed relay on the Indian power system during the blackout in July 2012. The comparison of the proposed relay with impedance-based relay and DB-based relay is explained in Section VII. The result and discussion are presented in Section VIII. Finally, the conlusion is presented in Section IX.

II. Mathematical Analysis of OOS Protection Scheme

The PMU at the generator bus can measure the magnitude and phase of positive-sequence voltages and currents, local frequency, local rate of change of frequency, and statuses of circuit breaker and switch synchronously. Figure 1 shows the schematic diagram of the PMU incorporated polygon-shaped OOS protection system. The advantage of PMU over the local measurement is that it can measure an absolute angle regarding the global timestamp or pure cosine wave. A positive-sequence impedance can be measured using PMU data, and is expressed as:

$$Z\angle\theta = \frac{|V|}{|I|}(\theta_1 - \theta_2) \tag{1}$$

where Z, V, and I are the positive-sequence impedance, voltage, and current, respectively; θ is the relative angle between V and I; and θ_1 and θ_2 are the absolute angles of V and I, respectively. In Fig. 1, f_g is the frequency of power generation; and G represents the synchronous generator.

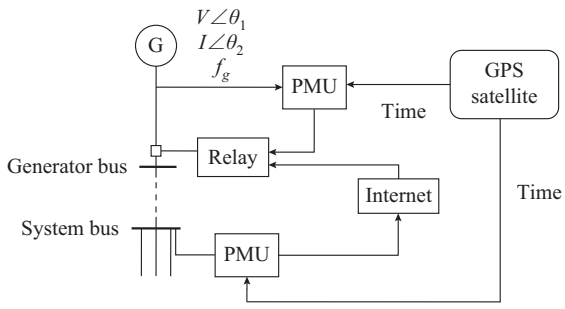

Fig. 1. PMU incorporated polygon-shaped OOS protection system.

The expression of a positive-sequence current and a positive-sequence voltage at the generator terminal is given as:

$$I\angle\theta_2 = \frac{E_g\angle\delta - E_s}{X_g + X_T + Z_s} \tag{2}$$

$$V\angle\theta_1 = E_g\angle\delta - X_g I\angle\theta_2 \tag{3}$$

where E_g is the voltage behind transient reactance of generator G; E_s is the system voltage; δ is the changing angle be-

tween the generator and system voltage; X_g is the equivalent reactance of the generator; X_T is the reactance of the transformer; and Z_s is the system impedance.

Substituting the value of $I\angle\theta_2$ into (3) yields:

$$V\angle\theta_1 = E_g\angle\delta - X_g\frac{E_g\angle\delta - E_s}{X_g + X_T + X_s} \tag{4}$$

Assume a special condition, where

$$\begin{cases} n = \dfrac{E_g}{E_s} = 1 \\ 1\angle\delta = \cos\delta + \mathrm{j}\sin\delta \end{cases} \tag{5}$$

From (5), the impedance observed by PMU data in real time is given by:

$$Z\angle\theta = (X_g + X_T + Z_s)n\frac{n - \cos\delta - \mathrm{j}\sin\delta}{(n-\cos\delta)^2 + \sin^2\delta} - X_g \tag{6}$$

From (6), it is clear that θ is propositional to δ, where δ is the angle between E_s and E_g, and $\theta = \theta_1 - \theta_2$.

If $\delta = 180°$ during pole slipping, $\theta = 180°$. Therefore, during pole slipping, θ is given by:

$$\theta_1 - \theta_2 = 180° \tag{7}$$

By using (7) during pole slipping, if an absolute angle of voltage θ_1 reaches 180°, an absolute angle of current θ_2 approaches 0°. After θ_2 approaches 0°, it crosses zero on the time axis and reaches −180° as shown in Fig. 2.

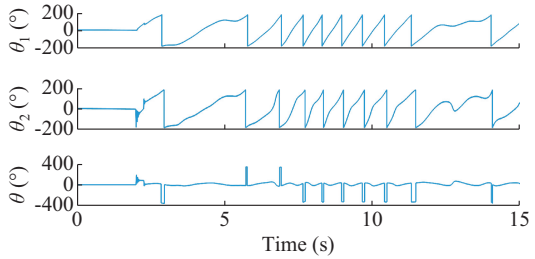

Fig. 2. θ_1, θ_2, and θ in variation with time during an event of unstable power swing.

At the time when the swing center arises near the generator transformer unit (GTU), there is a sudden change of frequency f. If the rate of change of frequency df/dt exceeds the threshold value, the generator may fall apart from the significant loads or the generator may fall apart completely [19]. In this paper, the threshold value of df/dt is set to be 1.5 Hz/s, which is dependent on the maximum permissible unbalanced power through the synchronous generator and df/dt relay settings. The value of df/dt is calculated in this work using (8) at terminal G_1 by allowing the maximum possible unbalanced power, which must produce the frequency variation less than the permissible range for grid frequency [20]. The permissible limit considered in the setting is ±3% referring to the Indian power grid code.

$$\frac{\mathrm{d}f}{\mathrm{d}t} = \frac{P_G - P_L}{2S_G H_G} f_s \tag{8}$$

where P_G is the output power of generation; P_L is the power load; f_s is the rated system frequency; S_G is the generator rating; and H_G is the inertia constant of generation plant.

The impedance trajectory of the power swing that passes 120° is generally not recoverable [12]. An associate generator breaker (GB) gets much stress with the OOS tripping from 120° to 180°. The switching of breaker after 270° produces lower stress on the GB.

Consider $E_g = E_s$ ($n = 1$) in (6) for the visualization of impedance trajectory, as shown in Fig. 3. In Fig. 3, point A is the intersection point between the right slope 2 R_{slope2} with horizontal line of resistance axis ($X = 0$); point B is the intersection point between the right slope 1 R_{slope1} with horizontal line of resistance axis ($X = 0$); point C is any point on the maximum reactance reach of the inner polygon; point D is any point on the maximum reactance reach of the outer polygon; D_1 and D_2 are the power swing angles at points A and B, respectively; and L_{slope1} and L_{slope2} are the left slopes 1 and 2, respectively. The actual swing characteristic differs from the special conditions. Thus, to detect the sophisticated and unusual swing in the case of PSS and increasing renewable penetration, a new polygon-shaped graphical characteristic is designed. The Kundur two-area system is considered as a test system in this paper, and its details are given in Appendix A [21]. The multi-band (MB) PSS with simplified settings, i.e., IEEE type PSS4B according to IEEE Std 421.5, works as PSS in the test system as shown in Fig. 4.

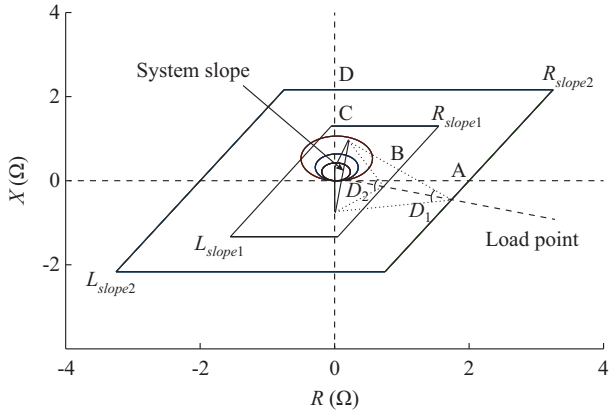

Fig. 3. Polygon-shaped graphical characteristic of proposed algorithm.

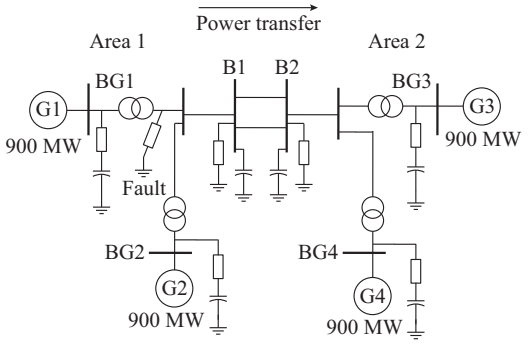

Fig. 4. A Kundur two-area system (test system).

III. PMU-INCORPORATED POLYGON-SHAPED OSS PROTECTION SCHEME

Figure 5 shows the flowchart of proposed PMU-incorporated polygon-shaped OOS protection scheme, and the proposed algorithm is as follows.

Step 1: at the generator bus, PMU continuously measures

the impedance $Z\angle\theta$. If the impedance trajectory crosses from the right slope 2 to 1, the timer starts and calculates T_1. For visualization, refer to Fig. 3.

Step 2: if $T_1 \geq T_s$, where T_s is the delay time, it indicates slow power swing due to sudden load change, load encroachment, or any other system power flow changes. If $T_1 < T_s$, it indicates fast power swing due to the fault.

Step 3: the graphical algorithm checks that either $Z\angle\theta$ passes through the system slope or it passes the left slope 2 from the right slope 2. It simultaneously checks whether $\theta >$ 270° using PMU. For the visualization of this condition, refer to Fig. 3. If both conditions explained in *Step 3* are satisfied in real time, the OOS pick-up condition is detected. The OOS tripping will be declared after *Step 4*.

Step 4: using PMU measurements at generator bus, the algorithm checks the following conditions: ① df/d$t > j$ (where j is the threshold value of df/dt, and for the test system, $j =$ 1.5 Hz/s); ② $V\angle\theta_1$ crossing zero; ③ $I\angle\theta_2$ crossing zero; and ④ θ passing the left slope 1.

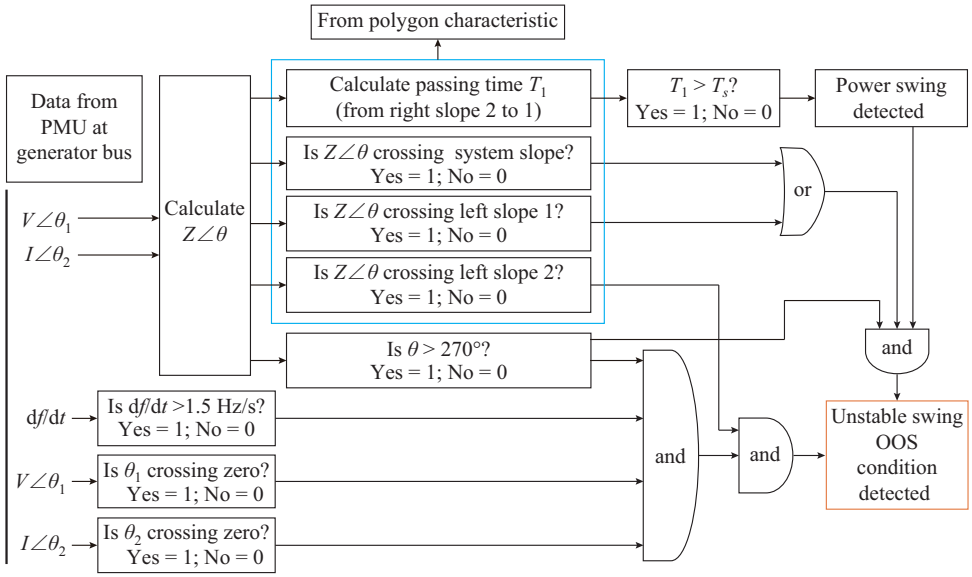

Fig. 5. Flowchart of proposed PMU-incorporated polygon-shaped OOS protection algorithm.

Finally, the OOS tripping declares if *Step 3* and *Step 4* are correct. Table I gives the setting and its calculation procedure for polygon-shaped characteristics using G_1 data of the Kundur two-area system, where Z_1, Z_2, and Z_3 represent zone 1, zone 2, and zone 3, respectively; Z_{GS} is the total impedance between generator to system; D_1 and D_2 are the entering angles at right slopes 1 and 2, respectively; f_{slip} is the slip frequency; and f_n is the nominal frequency.

TABLE I
SETTINGS OF POLYGON-SHAPED CHARACTERISTICS

Setting	Value	Calculation procedure
Radius of Z_1	0.4253 Ω	$80\%Z_{GS}$
Radius of Z_2	0.6380 Ω	$120\%Z_{GS}$
Radius of Z_3	1.0633 Ω	$200\%Z_{GS}$
$X_{d'}$	0.73315 Ω	Transient reactance
Distance of point A	2 Ω	Inside the maximum load
Distance of point B	0.79911 Ω	From point A, inside 35°
Distance of point D	1.46665 Ω	$2X_{d'}$
Distance of point C	1.333 Ω	From point D, inside 30°
Slope of lines A and B	tan 60°	At system line slope angle
X_T	0.3 Ω	From rating
Z_s	2.81 Ω	Assuming healthy system
T_s	0.025 s	$\frac{(D_2 - D_1) f_n}{f_{slip} \times 360°}$

IV. IMPLEMENTATION AND TESTING OF PROPOSED ALGORITHM

The three-phase short-circuit fault has been created just before GTU, as shown in Fig. 4. In this first event, the fault is removed before the critical clearing time (CCT) of the system. The results of the impedance trajectory in this case are shown in Fig. 6.

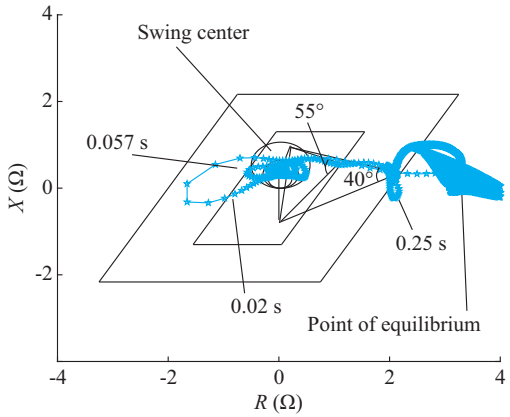

Fig. 6. Impedance trajectory of stable power swing due to swing center arising near GTU of G_1.

In the next event, the fault is removed after the CCT and the system becomes unstable, which is shown in Fig. 7.

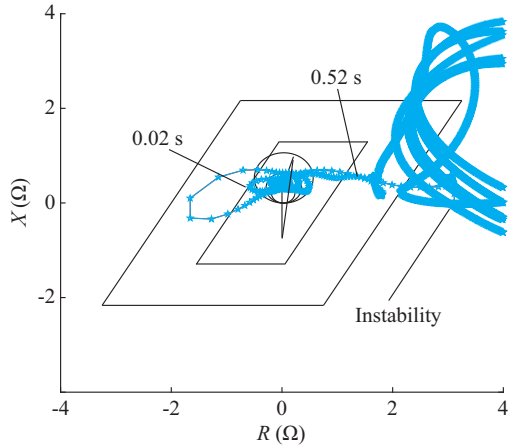

Fig. 7. Impedance trajectory of unstable power swing.

A. Event 1: Fault Removed Before CCT

The CCT for the three-phase fault located in Fig. 4 is 0.225 s, which is found by a simulation study. At $t=0$ s, the impedance point is outside the right slope 2. After 0.004 s, the impedance trajectory crosses the right slope 2, and in the next 0.003 s, it crosses the right slope 1. Thus, *Step 1* of the proposed algorithm is satisfied, and the timer calculates the time *T*. The result $T=0.0036\ \text{s}\leq T_s$ indicates a fast power swing from *Step 2*. After the fault clearance, the point comes right back near the previous load point after 0.25 s. The algorithm verifies that θ is crossing 270° after the fault is cleared, as shown in Fig. 8, and thus, the OOS pick-up is announced. Figure 6 shows the impedance trajectory.

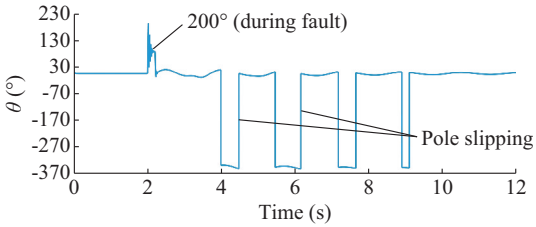

Fig. 8. Stable system after pole slipping.

Step 4 decides whether this complex swing is stable or not. In this event, conditions (2)-(4) of *Step 4* are satisfied but (1) is not satisfied. Hence, the OOS blocking is detected, and no tripping is announced. *Step 4* identifies it as a stable power swing. The decision taken by *Step 4* is verified as the system gains its equilibrium as shown in Fig. 6.

B. Event 2: Fault Removed After CCT

In this event, within 0.02 s after the fault, the swing passes the right slope 2 to the right slope 1 and moves back by crossing the left slope 1. The timer calculates the total time $T=0.0036\ \text{s}\leq T_s$, and therefore, *Step 2* indicates it as fast power swing due to the fault. *Step 3* of the proposed algorithm is satisfied very quickly in this event, and the OOS pick-up is announced. Now, *Step 4* decides the type of power swing. From Figs. 7 and 9, it can be observed that conditions (1)-(4) are satisfied. Finally, the OOS command is sent to the GB for rapid disconnection. It is interesting to note that the actual loss of synchronism due to angle separation is 3.92 s after the fault, but the proposed algorithm detects it 1 s before. Early detection is beneficial for decision-making to other relays, which are in co-ordination with the OOS relay. The decision is verified correctly as the diameter of the swing trajectory keeps on increasing as shown in Fig. 7.

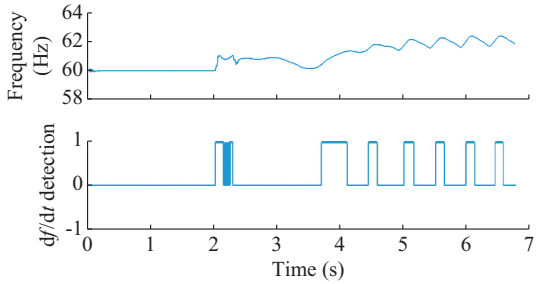

Fig. 9. Frequency and d*f*/d*t* detection in variation with time.

V. Testing of Proposed Algorithm for LG, LL, and Three-phase (LLL) Faults and Swing Center Arising Inside Generator

Different faults at a given location in Fig. 4 have different CCTs. The proposed algorithm is tested for LG, LL, and LLL faults at a given location. The CCTs are 0.7 s, 0.4 s, and 0.225 s for the LG, LL, and LLL faults, respectively. We simulate the swing center inside the generator by creating a 3-phase fault at the terminal of the generator.

Figure 10 shows the rotor angle deviation δ for different power swing conditions due to the LG, LL, and LLL faults. The rotor angle deviation increases as the fault clearing time increases, and for the fault removed before the CCT of the system, the deviation is less than 2.5 rad, which finally achieves the rotor angle stability with the action of PSS. When the LG, LL, and LLL faults are removed after the CCT, the rotor angle deviation is too high, which results in the first swing instability under the action of PSS.

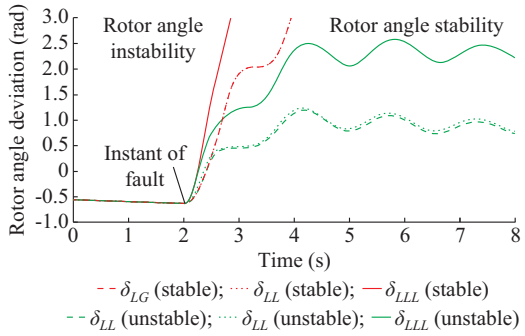

Fig. 10. Rotor angle deviation during power swing due to LG, LL, and LLL faults.

The rotor angle deviation is too high, which results in the first swing instability under the action of PSS. From Fig. 10, it is clear that LLL fault near the GTU of G_1 significantly affects the rotor angle stability and provides very less control margin compared with LL and LG faults near the GTU of G_1. Thus, the design of the OOS protection requires to consider the three-phase fault near the GTU of G_1 carefully. Fur-

thermore, the analysis of different power swings due to LL, LG, and LLL faults also shows that the speed variation of the generator has less margin in case of power swings than the transient faults. Table II shows the results of all cases of faults. Table III presents the settings calculated for DB scheme for comparison with the proposed algorithm.

TABLE II
COMPARISON OF PROPOSED ALGORITHM AND DB SCHEME IN DIFFERENT TRANSIENT EVENTS WITH ACTIVE PSS

Event	DB decision	Proposed algorithm
LLL fault (stable swing)	Incorrect	Correct
LLL fault (unstable swing)	Correct	Correct
LG fault (stable swing)	Incorrect	Correct
LG fault (unstable swing)	Correct	Correct
LL fault (unstable swing)	Correct	Correct
LL fault (stable swing)	Incorrect	Correct
Swing center in G_1 (unstable swing)	Correct	Correct

TABLE III
SETTINGS USED IN DB SCHEME

Type of setting	DB scheme
Radius of mho element from the origin	1.1 Ω
Outer right blinder	2 Ω
Inner right blinder	0.79 Ω
Outer left blinder	−2 Ω
Inner left blinder	−0.79 Ω
T_d	0.004 s

VI. PERFORMANCE TEST OF PROPOSED ALGORITHM

The performance test is divided into two parts: ① test under different levels of wind power penetration; ② test using the real physical system.

For the simulation system, we have designed the modified Kundur two-area system to find the effect of different levels of renewable penetration on the proposed OOS relay. Four identical doubly-fed induction generators (DFIGs) (type-4) are connected at buses BG1-BG4 such that the total power flow remains the same from area 1 to area 2 [8]. Figure 11 shows the modification in the Kundur two-area system to inject power from wind power sources (W1-W4) by making the power transfer the same as the original Kundur two-area system.

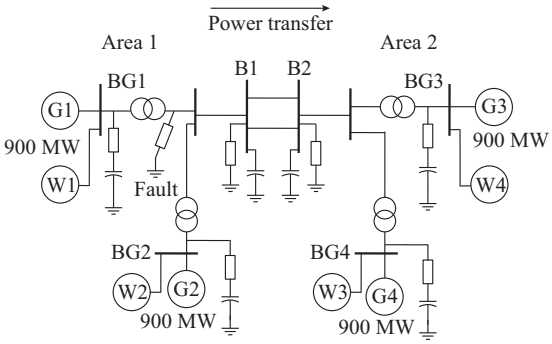

Fig. 11. A modified Kundur two-area system.

We have provided results by assessing the proposed algorithm on the real Indian power grid, which is shown in Fig. 12 as a simplified system just before the blackout. The Indian power grid experienced the blackout on July 30 (day 1) and 31 (day 2), 2012. We have used real PMU measurements of [22] and [23], which are shown in Fig. 13. We have also used the real PMU data collected from data logged at wide-area frequency measurement system (WAFMS) at Indian Institute of Technology-Mumbai (IIT-Mumbai) as the inputs to the proposed relay.

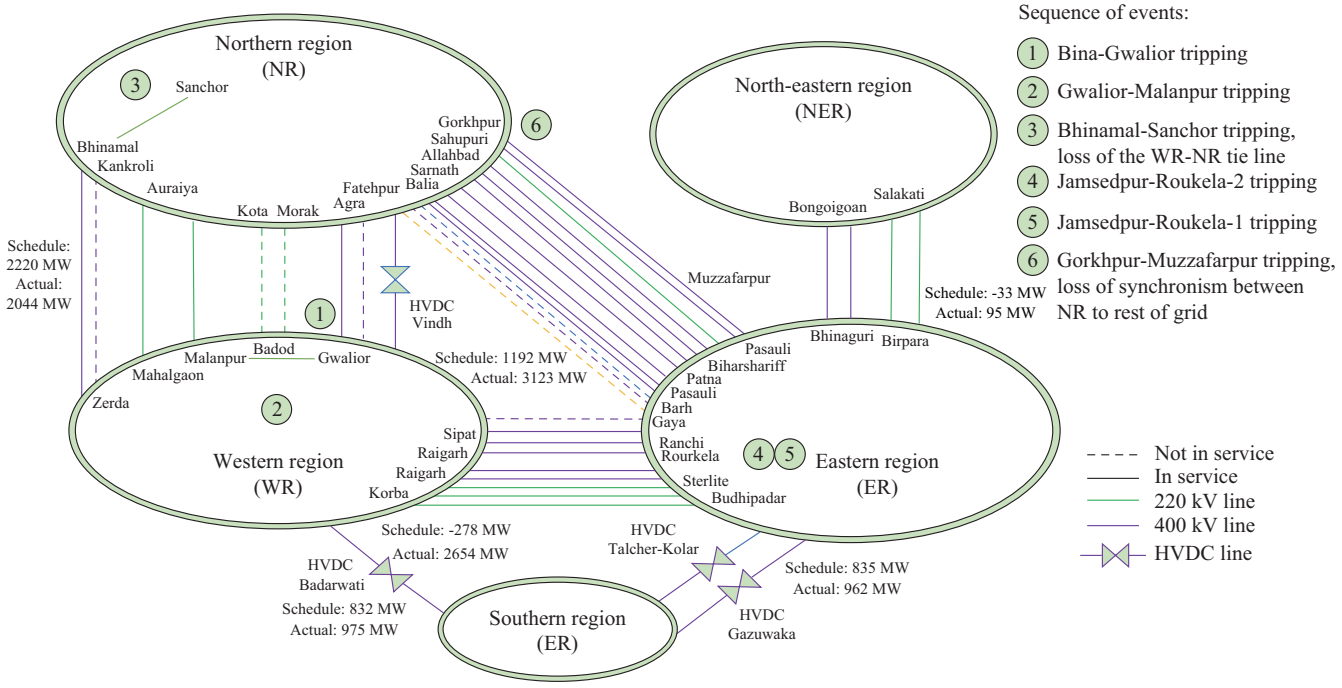

Fig. 12. Antecedent condition of Indian power grid on July 30, 2012.

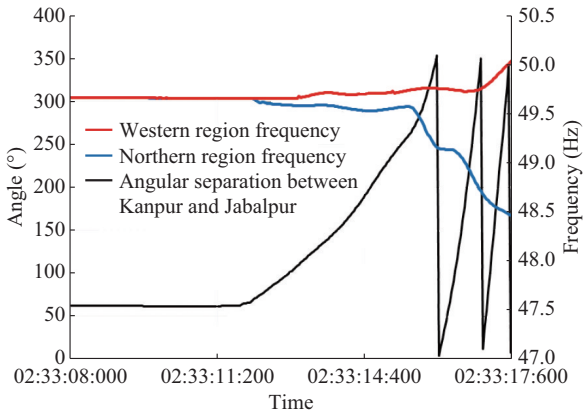

Fig. 13. Real PMU measurement on July 30, 2012.

A. Test at Different Levels of Renewable Power Penetration

The CCT of the system at the given location for three-phase fault keeps decreasing as the penetration of wind power increases. Table IV shows the tripping time with different levels of penetration. The impedance trajectory for different levels of penetration is shown in Fig. 14. The details of DFIG (type-4) are available in [24]. The proposed algorithm performs perfectly well under renewable integration. The proposed algorithm shows better performance when the system becomes weak due to significant renewable power injection. The changed path of impedance trajectory with the increment of renewable power does not require to change the threshold and slopes in the proposed algorithm.

TABLE IV
TRIPPING TIME OF PROPOSED ALGORITHM WITH DIFFERENT LEVELS OF RENEWABLE POWER PENETRATION

Penetration level (%)	Swing due disturbance	Tripping time (s)
7.6	Stable swing	No tripping
14.1	Stable swing	No tripping
21.2	Unstable swing	0.160
29.3	Unstable swing	0.060
35.4	Unstable swing	0.025

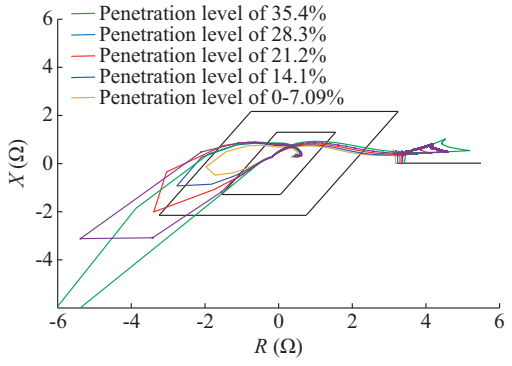

Fig. 14. Impedance trajectory at different levels of renewable power penetration.

The power swing characteristics are influenced by renewable power energy sources (RPESs) and exhibit an unstable internal impedance. Also, the intigration of RPES has altered the reactance and resistance reach, as shown in Fig. 14. This is due to limited current amplitude, current frequency offset, and controlled current phase angle due to inverter-driven sources, which are different from the synchronous-generator-based sources.

B. Test Using Real Physical System

The different successive disturbing events on July 30, 2012 to the Indian power grid result in a blackout. It is observed that before the blackout, the number of transmission lines is not available, or in forced or planned outages, or kept out to control high voltages. The out-of-service lines are shown as dotted lines in Fig. 12. The number of out-of-service lines results in a weak inter-region transmission network with high demand in the NR. Figure 12 shows 220 kV lines in green color, 400 kV lines in purple color, and sequence of events with numbers. Also, Fig. 12 shows the condition before the disturbance with the scheduled and actual power flows between different regions of the Indian power grid. It can be observed that the grid is under stress condition before the blackout. Before complete area separation between WR-ER-NR to NR, the events are described as follows [23]:

1) Event 1 at 02:33:11:907 a.m.: 400 kV Bina-Gwalior-1 line tripping because of zone 3 tripping and 220 kV Gwalior-Malanpur-1 transmission line tripping, which causes Malanpur and Mehgaon loads to be fed from the NR system.

2) Event 2 at 02:33:13:438 a.m.: 220 kV Bhinmal-Sanchor line tripping on zone 1 due to power swing.

3) Event 3 at 02:33:13:927 a.m.: 400 kV Jamshedpur-Rourkela line 2 tripping on zone 3 distance relay.

4) Event 4 at 02:33:13:996 a.m.: 400 kV Jamshedpur-Rourkela line 1 tripping on zone 3 distance relay.

5) Event 5 at 02:33:15:400 a.m.: 400 kV Gorakhpur-Muzaffarpur circuit 2 tripping on power swing.

The above sequence is shown in Fig. 12 with its location in the Indian power grid. The assessment of the proposed algorithm for the above events is described as follows.

Step 1: considering the NR end at 02:33:15:400 a.m., on 400 kV Gorakhpur-Muzaffarpur circuit 2, the measured phase voltages are 123 kV, 116 kV, 115 kV, and currents are 2.42 kA, 2.48 kA, 2.45 kA for the red-yellow-blue (RYB) phase, respectively. The calculated impedance for the control area at the NR end at this time is in order of 0.65 Ω. Hence, the impedance crosses the right slope 2 to 1 in the proposed relay.

Step 2: it detects the power swing due to load change at 02:33:15:400 a.m. due to slow trajectory which is reaching to the system slope.

Step 3: $\theta > 270°$ from PMU measurement is not satisfied at 02:33:13:996 a.m. as the angle difference of WR-ER-NR to NR does not exceed 270°, as shown in Fig. 13. The phase difference less than 270° implies that the relative angle θ does not exceed the set value, neither, which means that till 02:33:13:996 a.m., the proposed algorithm is immune to trip the control area of NR at 2:33:13:996 a.m., which is the desired operation. At 2:33:15:996 a.m., $\theta > 270°$ is satisfied, and *Step 3* announces the OOS pick-up as per the proposed

relay logic.

Step 4: it is explained with each condition as follows.

1) $df/dt > j$ (considering $j = 1.5$ Hz/s) is true at 2:33:11:800 a.m., because as per our test, by using real measurement data logged at WAFMS of IIT-Mumbai, $df/dt > 1.5$ Hz/s is triggered at 2:33:11:800 a.m. on the NR end.

2) $V\angle\theta_1$ crosses zero at 02:33:15:400 a.m. on the NR end.

3) $I\angle\theta_2$ also crosses zero at 02:33:15:400 a.m. on the NR end.

4) θ crosses 270° at 02:33:15:400 a.m. on the NR end.

As per the proposed algorithm, the OOS condition is identified at 02:33:15:400 a.m. for NR. The inquiry report has also found that the actual separation of NR from WR-ER-NR occurrs at around 02:33:15:542 a.m. [23].

VII. Comparison of Proposed Algorithm with Existing Ones

The proposed algorithm shows excellent reliability as it uses a balanced combination of direct and indirect measurements for power swing detection compared with the existing schemes such as the DB and impedance-based schemes. Table V shows the contribution of the proposed algorithm in terms of performance compared with the existing ones. The impedance-based scheme alone is highly unreliable under the present power swing conditions. If the relay reach of the impedance-based relay is set high, it may trip for stable swing, and if the relay reach is set too small, it is mal-operated for unstable swings [21]. In the modern power system, the resistance and reactance reaches are subjected to the variation of renewable integration based on the analysis of Fig. 14. The DB scheme is less reliable as it is based on a blinder, which measures the rate of change of impedance. However, the rate of change of impedance is variable when the system uses PSS. The results of Table II indicate that the DB scheme is not much reliable. Also, both schemes are not adaptable for the same reason as discussed above. For the comparison of the accuracy of the proposed relay and existing ones, we have considered three criteria: ① detection of swing; ② time of OOS detection; ③ detection at other places of generator location. According to the above three aspects, the impedance-based relay performance is inferior and mal-operated frequently [21], where the DB scheme is better than the impedance-based scheme for the detection of unstable power swing. However, the DB scheme is mal-operated for a stable power swing as per the results of Table II. The results of Tables II and IV show that the proposed relay is accurately operated just before the actual loss of stability. The impedance-based method has no provision to identify symmetrical fault from power swing [21], wheras the DB and the proposed algorithm have the ability to identify three-phase fault from swing. However, the results in Table II show that the DB scheme is not that accurate due to its existing methodology. Further, the effect of PSS does not affect the performance of the proposed algorithm.

TABLE V
Performance Comparison of Proposed Algorithm with Existing Ones

Algorithm or scheme	Performance					
	Reliability	Adaptability	Accuracy	Detection of symmetrical fault	Detection of fault during swing	Effect of PSS
Impedance-based	Less	Not adaptable	Less	Not accurate	Not possible	More
DB	Average	Not adaptable	Average	Not accurate	Not possible	More
Proposed	Excellent	Adaptable	Excellent	Accurate	Possible	Not affected

VIII. Results and Discussion

The effect of the LG fault on CCT with different levels of penetration is shown in Table VI.

TABLE VI
Effect of Renewable Power Penetration on CCT of System for LG Fault

Penetration level (%)	CCT of system (s)
0	0.60
8	0.55
36	0.41
52	0.20
58	0.15
62	0.15

The CCT of the LG fault is significantly reduced with 50% renewable power penetration. The proposed algorithm produces the correct OOS tripping when the system becomes unstable due to the reduction of CCT, and remains immune when the swing is stable at the same fault duration with different levels of penetration. The proposed OOS algorithm adapts the renewable power environment and detects unstable swing faster compared with the system without renewable power penetration.

The LG fault more than CCT is applied near GTU of G1, as shown in Fig. 4. The proposed algorithm gives a decision after 0.32 s of fault clearance wheras the actual loss of synchronism occurs after 1.82 s of fault clearance. The DB scheme detects it faster than the proposed algorithm, less than 0.1 s of fault clearance. However, the algorithm needs to take enough time to decide the swing nature. The OOS triping signal must be sent to the generator before the actual loss of synchronism occurs. Thus, there will be available time for the island action. The DB scheme gives false tripping for stable power swing produced due to transient LG fault. The proposed algorithm proves to be reliable here and does not produce an OOS tripping signal in a stable power swing event. Figure 15 shows the impedance trajectory in

the proposed algorithm and DB scheme, respectively, for an unstable power swing due to LG fault.

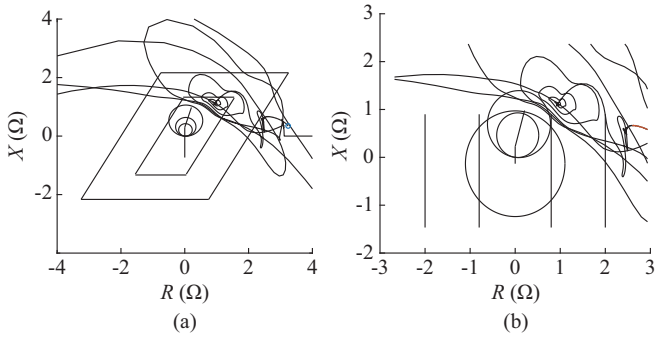

Fig. 15. Impedance trajectory for LG fault in proposed algorithm and DB scheme of unstable swing. (a) Proposed algorithm. (b) DB scheme.

Figure 16 shows the unstable impedance swing due to LL fault that arises near GTU of G_1 and reverses its direction, which seems like the stable swing. The previous confusing power swing of the LL fault is due to the effect of PSS working during the fault. For the stable power swing produced due to LL fault, the DB scheme gives unreal operation, and the proposed algorithm gives a correct decision.

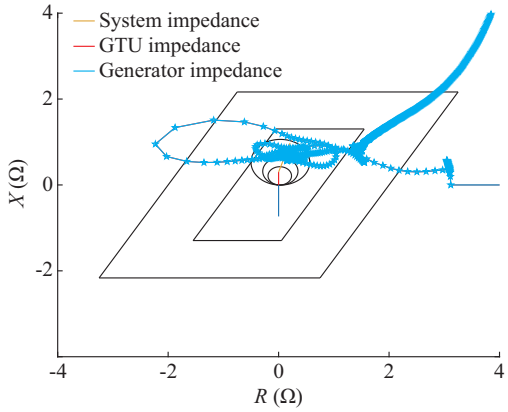

Fig. 16. Impedance trajectory for LL fault of unstable swing.

Figure 17 shows the rotor angle oscillations of generator G1 compared with G2, G3, and G4 that are not separated. The system achieves stability after the LL fault, and no loss of synchronism occurs. The proposed algorithm issues no OOS tripping signal and DB scheme issues a false tripping command, as shown in Fig. 17. The system, which is stable with 0% to 14% renewable power penetration, becomes unstable with 14% to 35% renewable power penetration for the same disturbance at the same location. The proposed relay gives the correct OOS tripping signal under unstable power swing after 14% renewable power penetration, and remains immune for stable power swing up to 0% to 14% penetration levels.

The swing center that arises inside the generator is simulated by applying a three-phase fault at the terminal of generator 1. The swing trajectory is somewhat more dangerous when arising inside the generator, and therefore, the proposed algorithm detects it faster. The fault is applied at 2 s. The proposed algorithm gives the trip command after 0.106 s of fault clearance, and the actual loss of synchronism is after 0.525 s. Figure 18 shows the comparison of OOS tripping time of DB scheme and the proposed algorithm. The DB scheme is not able to handle the severity of the fault. It takes more time in this case and gives OOS tripping after 0.558 s. The assessment of the proposed algorithm using real field data shows that the proposed algorithm has the capability to detect the loss of synchronism at the correct time, which prevents the generators from being damaged due to power swings.

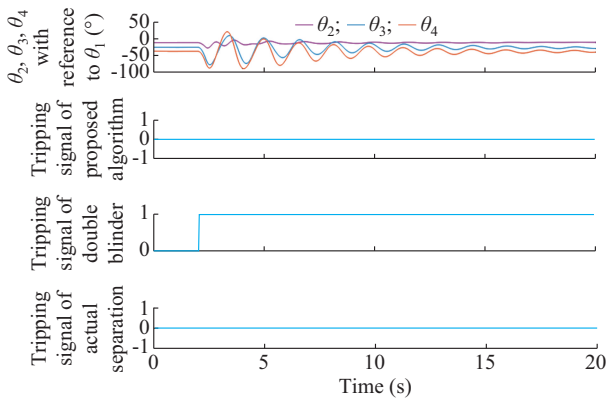

Fig. 17. Untrue operation of DB scheme in stable power swing due to LL fault.

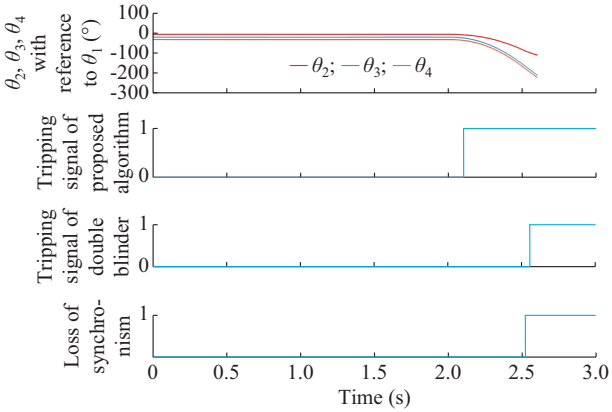

Fig. 18. Tripping time comparison with DB scheme when swing center arises inside generator.

IX. Conclusion

The transient events of modern power system with PSS in use can produce well-damped power oscillations as well as power swings which are much more challenging to detect. The PMU-based polygon-shaped graphical logic proposed in the paper accurately performs the task and detects complex power swings. The system is able to attain stability after one pole slipped in some events where the DB scheme mal-operates. The DB scheme is not reliable with PSS-enabled power systems or under renewable integration. Further, the DB scheme requires modifications of blinders and time delays to operate correctly under different power swing conditions.

The proposed algorithm is advantageous when a synchronous generator or group of generators is/are required to be protected from unstable power swings. The proposed algo-

rithm gives faster tripping when different levels of renewable power penetration control the unstable power swing. The impedance trajectory travels more distance from right to left with the increased wind power penetration for the same fault type, duration, and location. The result clarifies that the proposed algorithm is speedy and correct when the swing center comes inside the large generator. The proposed OOS relay does not require the revision of settings when system conditions are changed. The PMU data incorporated with a novel graphical scheme makes the algorithm adaptive in modern power system.

APPENDIX A

The system consists of two identical areas connected with very sensitive tie lines. Each area with two generator unit has a rated capacity and voltage of 900 MVA and 20 kV, respectively.

The generator parameters at rated capacity and voltage are as follows: $X_d = 1.8$ p.u.; $X_q = 1.7$ p.u.; $X_l = 0.2$ p.u.; $X_d' = 0.3$ p.u.; $X_q' = 0.55$ p.u.; $X_d'' = 0.25$ p.u.; $X_q'' = 0.25$ p.u.; $R_a = 0.0025$ p. u.; $T_{d0}' = 8.0$ s; $T_{q0}' = 0.4$ s; $T_{d0}'' = 0.03$ s; $T_{q0}'' = 0.05$ s; $A_{Sat} = 0.015$ p.u.; $B_{Sat} = 9.6$ p.u.; $\psi_{T1} = 0.9$ p.u.; $H = 6.5$ p.u. (for G1 and G2); $H = 6.175$ p.u. (for G3 and G4); $K_D = 0$.

For each step-up transformer, $Z_T = (0 + j0.15)$p.u. for the 900 MVA and 20/230 kV base, and the off-nominal ratio is 1.0 p.u.. For the transmission line, $r = 0.0001$ p.u./km; $x_L = 0.001$ p.u./km; $b_C = 0.00175$ p.u./km.

The system operates with area 1 exporting 400 MW to area 2, and the generation units are loaded as follows:

1) G1: $P_1 = 700$ MW; $Q_1 = 185$ Mvar; and $E_{t1} = 1.03$ p.u. (20.2°)

2) G2: $P_2 = 700$ MW; $Q_2 = 235$ Mvar; and $E_{t2} = 1.01$ p.u. (10.5°)

3) G3: $P_3 = 719$ MW; $Q_3 = 176$ Mvar; and $E_{t3} = 1.03$ p.u. (−6.8°)

4) G4: $P_4 = 700$ MW; $Q_4 = 202$ Mvar; and $E_{t4} = 1.01$ p.u. (−17.0°)

The loads and reactive power by shunt capacitors for bus 7 are: $P_L = 967$ MW; $Q_L = 100$ Mvar; and $Q_c = 200$ Mvar. For bus 9: $P_L = 1767$ MW; $Q_L = 100$ Mvar; and $Q_c = 350$ Mvar.

REFERENCES

[1] M. K. Gunasegaran, C. Tan, A. H. A. Bakar *et al.*, "Progress on power swing blocking schemes and the impact of renewable energy on power swing characteristics: a review," *Renewable and Sustainable Energy Reviews*, vol. 52, pp. 280-288, Dec. 2015.

[2] N. Ayer and R. Gokaraju, "Online application of local OOS protection and graph theory for controlled islanding," *IEEE Transactions on Smart Grid*, vol. 11, no. 3, pp. 1822-1832, May 2020.

[3] J. Machowski, "Selectivity of power system protections at power swings in power system," *Acta Energetica*, vol. 13, no. 4, pp. 96-111, Dec. 2012.

[4] J. Machowski, Z. Lubosny, J. W. Bialek *et al*., *Power System Dynamics: Stability and Control*. Hoboken: John Wiley & Sons, 2020.

[5] S. Choudhary and F. B. Sharma, "Small signal stability analysis of renewable source connected power system and identification of oscillatory modes using wavelet transform," in *Proceedings of 2015 International Conference on Smart Grid and Clean Energy Technologies (ICSGCE)*, Offenburg, Germany, Oct. 2015, pp. 23-29.

[6] J. L. Blackburn and T. J. Domin, *Protective Relaying: Principles and Applications.* London: Routledge & CRC Press, 2014.

[7] V. Ambekar and S. Dambhare, "Comparative evaluation of out of step detection schemes for distance relays," in *Proceedings of 2012 IEEE 5th Power India Conference*, Murthal, India, Dec. 2012, pp. 1-6.

[8] G. Liu, S. Azizi, M. Sun *et al.*, "Performance of OOS tripping protection under renewable integration," *The Journal of Engineering*, vol. 2018, no. 15, pp. 1216-1222, Jul. 2018.

[9] A. Haddadi, I. Kocar, U. Karaagac *et al.*, "Impact of wind generation on power swing protection," *IEEE Transactions on Power Delivery*, vol. 34, no. 3, pp. 1118-1128, Jun. 2019.

[10] P. Regulski, W. Rebizant, M. Kereit *et al.*, "PMU-based generator out-of-step protection," *IFAC-PapersOnLine*, vol. 51, no. 28, pp. 79-84, Jan. 2018.

[11] S. A. Lavand and S. A. Soman, "Predictive analytic to supervise zone 1 of distance relay using synchrophasors," *IEEE Transactions on Power Delivery*, vol. 31, no. 4, pp. 1844-1854, Aug. 2016.

[12] D. Reimert, *Protective Relaying for Power Generation Systems*. London: CRC/Taylor & Francis, 2006.

[13] N. Kumar, D. R. Nagaraja, and H. P. Khincha, "A smart and adaptive scheme for generator out of step protection," in *Proceedings of 2015 IEEE Innovative Smart Grid Technologies - Asia (ISGT ASIA)*, Bangkok, Thailand, Nov. 2015, pp. 1-6.

[14] A. G. Phadke and J. S. Thorp, *Synchronized Phasor Measurements and Their Applications*, 2nd ed. Boston: Springer, 2017.

[15] S. Zhang and Y. Zhang, "A novel OOS splitting protection based on the wide area information," *IEEE Transactions on Smart Grid*, vol. 8, no. 1, pp. 41-51, Jan. 2017.

[16] R. Franco, C. Sena, G. N. Taranto *et al*., "Using synchrophasors for controlled islanding–a prospective application for the Uruguayan power system," *IEEE Transactions on Power Systems*, vol. 28, no. 2, pp. 2016-2024, May 2013.

[17] H. Zare, H. Yaghobi, and Y. Alinejad-Beromi, "Adaptive concept of controlled islanding in power systems for wide-area OOS prediction of synchronous generators based on adaptive tripping index," *IET Generation, Transmission & Distribution*, vol. 12, no. 16, pp. 3829-3836, Sept. 2018.

[18] M. A. M. Ariff and B. C. Pal, "Adaptive protection and control in the power system for wide-area blackout prevention," *IEEE Transactions on Power Delivery*, vol. 31, no. 4, pp. 1815-1825, Aug. 2016.

[19] A. S. Elansari, M. F. Edrah, and S. M. Khaled, "Improve transient frequency response by adjusting generators' over frequency relays," in *Proceedings of 2012 IEEE International Conference on Power and Energy (PECon)*, Kota Kinabalu, Malaysia, Dec. 2012, pp. 458-463.

[20] P. Gupta, R. S. Bhatia, and D. K. Jain, "Active ROCOF relay for islanding detection," *IEEE Transactions on Power Delivery*, vol. 32, no. 1, pp. 420-429, Feb. 2017.

[21] P. Kundur, *Power System Stability and Control*. New York: McGraw Hill, 1994.

[22] Central Electricity Regulatory Commission. (2012, Aug.). Grid disturbance on 30th July 2012 and grid disturbance on 31st July 2012. [Online]. Available: http://cercind. gov. in/2012/orders/Final_Report_Grid_Disturbance.pdf

[23] Ministry of Power of India. (2012, Aug.). Report of the enquiry committee on grid disturbance in northern region on 30 July 2012 and in northern, eastern and north-eastern region on 31 July 2012 New Delhi, India. [Online]. Available: http://powermin.nic.in/upload/pdf/GRIDENQREP16812.pdf

[24] A. S. Trevisan, A. A. El-Deib, R. Gagnon *et al*., "Field validated generic emt-type model of a full converter wind turbine based on a gearless externally excited synchronous generator," *IEEE Transactions on Power Delivery*, vol. 33, no. 5, pp. 2284-2293, Oct. 2018.

Jigneshkumar P. Desai received the B.E. degree in electrical engineering from Veer Narmad South Gujarat University (VNSGU), Surat, India, in 2010, and the M.Tech. degree in electrical engineering from the Nirma University (NU), Ahmadabad, India, in 2013. Currently, he is pursuing his Ph.D. degree in electrical engineering from the Gujarat Technological University (GTU), Ahmadabad, India. He has more than seven years of teaching experience. He is currently working as an Assistant Professor in the Electrical Engineering Department, Sarvajanik College of Engineering and Technology, Surat, India. His current research interests include modern power system protection, power system stability, and artificial intelligence in the power system.

Vijay H. Makwana received his B.E. (electrical) and M.E. (electrical power system) degrees from BVM Engineering College, Sardar Patel University, Vallabh Vidyanagar, Gujarat, India, in 1999 and 2002, respectively. He received his Ph.D. (electrical) degree from Sardar Patel University, Vallabh

Vidyanagar, India, in 2013. He has more than 17 years of teaching experience. Currently, he is working as a Professor in the Department of Electrical Engineering, G. H. Patel College of Engineering and Technology, Vallabh Vidyanagar, India. He has published seven papers in various international peer-reviewed journals. He has written a book Power System Protection and Switchgear published by Tata Mc-Graw Hill, India, in 2010. He has also written a monograph on Transmission Line Protection Using Digital Technology published by Springer, in 2016. His research interests include power system protection, power system stability and control, power system modeling and simulation, reactive power compensation and flexible alternating current transmission system (FACTS).